

SANDIA REPORT

SAND91-0657 • UC-706

Unlimited Release

Printed May 1991

FINAL COPY C.2

Sandia's New HyperVelocity Launcher—HVL

L. C. Chhabildas, L. M. Barker, J. R. Asay, T. G. Trucano, G. I. Kerley

Prepared by
Sandia National Laboratories
Albuquerque, New Mexico 87185 and Livermore, California 94550
for the United States Department of Energy
under Contract DE-AC04-76DP00789



SAND91-0657
0002
UNCLASSIFIED

05/91
32P STAC

Issued by Sandia National Laboratories, operated for the United States Department of Energy by Sandia Corporation.

NOTICE: This report was prepared as an account of work sponsored by an agency of the United States Government. Neither the United States Government nor any agency thereof, nor any of their employees, nor any of their contractors, subcontractors, or their employees, makes any warranty, express or implied, or assumes any legal liability or responsibility for the accuracy, completeness, or usefulness of any information, apparatus, product, or process disclosed, or represents that its use would not infringe privately owned rights. Reference herein to any specific commercial product, process, or service by trade name, trademark, manufacturer, or otherwise, does not necessarily constitute or imply its endorsement, recommendation, or favoring by the United States Government, any agency thereof or any of their contractors or subcontractors. The views and opinions expressed herein do not necessarily state or reflect those of the United States Government, any agency thereof or any of their contractors.

Printed in the United States of America. This report has been reproduced directly from the best available copy.

Available to DOE and DOE contractors from
Office of Scientific and Technical Information
PO Box 62
Oak Ridge, TN 37831
Prices available from (615) 576-8401, FTS 626-8401

Available to the public from
National Technical Information Service
US Department of Commerce
5285 Port Royal Rd
Springfield, VA 22161

NTIS price codes
Printed copy: A03
Microfiche copy: A01

SAND91-0657
Unlimited Release
Printed, May 1991

Sandia's New *Hyper Velocity Launcher – HVL*

L. C. Chhabildas, L. M. Barker, J. R. Asay
T. G. Trucano, G. I. Kerley

*Experimental Impact Physics Division
Sandia National Laboratories
Albuquerque, New Mexico 87185*

ABSTRACT

A systematic study is described which addresses the technical issues associated with launching flier-plates intact to hypervelocities. First, very high pressures are needed to launch the flier plates to hypervelocities, and second this high pressure loading must be uniform and nearly shockless. To achieve both these criteria, a graded-density material referred to as a "pillow" is used to impact a flier plate. When this graded-density material is used to impact a flier plate at high velocities on a two-stage light-gas gun, nearly shockless megabar pressure pulses are introduced into the flier plate. Since the loading on the flier plate is shockless, melting of the flier plate is prevented. This technique has been used to launch a 2-mm thick titanium alloy (Ti-6Al-4V) plate to a velocity of 8.1 km/s, and a 1-mm thick aluminum alloy (6061-T6) plate to a velocity of 10.4 km/s. A method is described by which the flier plate velocities could be further augmented to velocities approaching 14 km/s.

Contents

1	INTRODUCTION	3
2	EXPERIMENTAL TECHNIQUE	4
2.1	Barrel Extensions	4
2.2	Flier-Plate Configuration	6
2.3	Projectile Design	6
2.4	Diagnostics	7
3	RESULTS	7
3.1	One-Dimensional Numerical Simulation	13
3.2	Two-Dimensional Simulations	13
3.3	Velocity Enhancement	23
4	SUMMARY	26
5	ACKNOWLEDGMENTS	26
6	REFERENCES	27

1 INTRODUCTION

There is continued interest in developing laboratory techniques to accelerate plates to hypervelocities for the purpose of determining the equation of state of materials at extremely high pressures, temperatures, and strain rates. A combination of such experimental hypervelocity launch techniques with improved understanding of material behavior at extreme pressures and temperatures would be useful in addressing the physical processes associated with a variety of hypervelocity impact events such as meteorite impact or lethality studies.

Current technology allows the use of two-stage smooth-bore guns [1] to accelerate sabot materials with a facing plate having a total mass of ~ 15 to 20 gm to velocities approaching 8 km/s. The acceleration in the second stage of the two-stage light-gas gun which is required to achieve such high velocities is 10^9 cm/s². If the operating parameters for the gun are not optimized, there is a potential for sabot break-up. The concept of staging has also been applied to explosive systems [2], with the final velocity of 1 mm stainless steel flier-plates approaching 7 to 9 km/s over a run distance of 20 mm. Longer run distances, however, do have a potential of fragmenting the plates [2]. Another approach to achieving high velocities is to use a rail-gun in which a magnetically driven plasma is used to drive a projectile carrying a nose plate. More recently, concepts of using a two-stage light-gas gun to inject a projectile into the rail gun at velocities up to 8 km/s have been explored [3]. Once the projectile is in the rail gun, the magnetically driven plasma pressure (approximately 0.3 GPa) is expected to further enhance the velocity by an additional 2 to 7 km/s [3].

In all of the above systems, gas pressures (*i.e.*, hydrogen gas in the two-stage light-gas gun, propellant gaseous products in the explosive systems, and plasma gases in the rail gun) are used to drive projectiles to high velocities. In most of these approaches [1-3], the driving gas pressure is sufficiently low (~ 1 GPa), so that the projectile nose plate stays elastic and undeformed throughout the acceleration process. It would seem, therefore, that very high driving gas pressure [4,5] (tens or hundreds of GPa), would be necessary to accelerate flier plates to hypervelocities. However, since the flier-plate is now subjected to driving gas pressures which are orders of magnitude above its elastic limit severe deformation will occur. Also, because the flier plate has limited tensile strength [6,7] it will have a tendency to fragment. Fragmentation can be minimized by selecting a material which has a large normalized spall strength [6,7] and is therefore relatively resistant to fragmentation. Nevertheless, if the non-uniformity in gas pressure loading [6,7] over the entire face of the flier plate is sufficiently large flier fragmentation may still occur.

In all of the above examples, gas pressures are used to accelerate plates to high velocities since they provide a convenient means by which either the projectile or a flier plate is accelerated shocklessly. Shockless acceleration of the flier plate is particularly crucial if gas pressures approaching hundreds of GPa are to be used as a driving medium. If the duration (rise-time) of the pressure pulse were too small, a shock will form within

the flier plate. The energy dissipated due to shock heating would result in a substantial temperature increase causing the plate to melt. This is especially true for low melting materials such as aluminum in which shock-induced melting occurs at ~ 120 GPa [8,9]. Since the energy dissipation in the material under shockless loading is much less than under shock loading[10], a pressure pulse having a finite rise-time is better suited for accelerating plates to hypervelocities. Shockless acceleration of the plate is therefore an important criterion for preventing shock-induced heating and subsequent melting of the flier during the acceleration process[7].

It is the purpose of this paper to describe an alternate loading technique that can be used to accelerate flier plates to hypervelocities. The technique eliminates the use of high pressure gas, a major source of non-uniform loading on the flier-plate. As mentioned above, there are two main requirements to launch flier plates to hypervelocities. First, very high pressures are needed to launch the flier plate, and second this loading must be nearly shockless and uniform over its entire surface. To achieve both these criteria, a graded-density material [11] referred to as a "pillow" is used to impact the flier plate. When this graded-density material is used to impact a flier plate at high velocities on a two-stage light-gas gun [10-11], nearly shockless megabar pressure pulses are introduced into the flier plate. Since the loading on the flier plate is shockless, excessive heating is minimized to prevent melting of the flier plate[10]. This method has been used to launch a 2-mm thick titanium alloy (Ti-6Al-4V) plate to a velocity of 8.1 km/s, and a 1-mm thick aluminum alloy (6061-T6) plate to a velocity of 10.4 km/s. With further improvements to this technique launch velocities approaching 14 km/s are expected.

2 EXPERIMENTAL TECHNIQUE

This section briefly describes the experimental techniques employed to augment the launch capabilities of Sandia's 28 mm bore two-stage light-gas gun. (For the purpose of this discussion a velocity in excess of 7 km/s for gram size masses is defined to be hypervelocity.) The experimental impact configuration is indicated in Figure 1. The two-stage light-gas gun used in these studies had a bore diameter of 28.6 mm. As indicated in the figure, a two-stage light-gas gun projectile which has a pillow facing is made to impact a thin flier plate located at the muzzle end of the barrel. Implementation of these techniques require that the barrel of the two-stage light-gas gun be extended, and that the flier plate be laterally confined to minimize two-dimensional effects.

2.1 Barrel Extensions

Practical considerations dictate the use of three short extensions to the original gun barrel muzzle. (Each barrel extension has a bore diameter of 28.6 mm, and is the same as the bore diameter of the actual gun barrel.) The details of the modifications to the two-stage

light-gas gun barrel are shown in Figure 2. The first extension provides an isolation of the experiment from the gun recoil by the use of a slip joint at the muzzle of the gun. The extension is aligned concentric with the gun barrel using an expanding mandrel technique. The inside of the mandrel is hydraulically pressurized, causing it to expand and hold the barrel extension exactly concentric with the barrel. Setscrews are then tightened to preserve the alignment after which the expanding mandrel is depressurized and removed.

The flier-plate is situated in the second extension, called the target fixture (See Figure 2). One purpose of the target fixture is to provide inertial lateral confinement of the megabar pressures developed between the graded-density impactor and the flier-plate. Hence, the target fixture is made of a high density tungsten alloy. This segment is an expendable item and is designed to be replaced at minimal expense. The target fixture is aligned with the barrel extension using the same expanding mandrel technique mentioned above.

The downstream end of the target fixture is fitted with a barrel extension consisting of an aluminum tube. Its primary purpose is to provide collimation as the flier plate exits the target fixture. An aluminum tube is used because it is transparent to (600 KeV) X-rays which are used to infer the flier plate velocity and integrity.

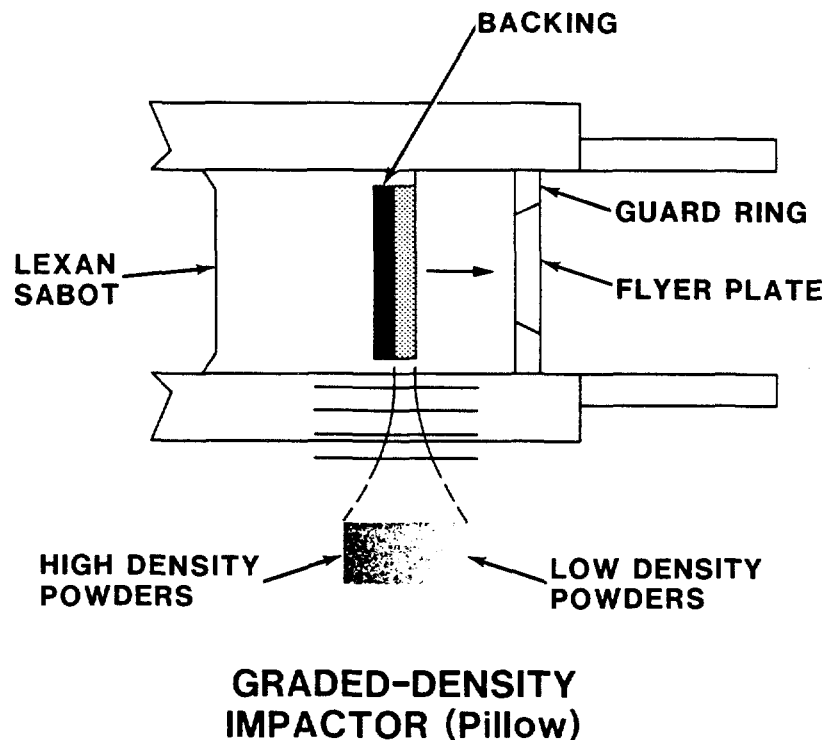


Figure 1. Schematic of a Graded-Density Impactor/Flier-Plate Experiment.

2.2 Flier-Plate Configuration

As shown in Figure 1, the flier plate used in these experiments consists of a center plate made to fit exactly into a guard ring. The outside diameter of the guard ring used in these studies was 28.6 mm, while the inner diameter of the guard ring and the diameter of the center plate was 19 mm. The thickness of each flier plate is listed in Table I. Two-dimensional effects due to radial release waves (generated upon impact) emanating from the edges of the plate would cause a velocity gradient across the radius of the plate. Large velocity gradients across the radius of the plate would cause the flier plate to bend and, perhaps, even fragment. The guard ring geometry indicated in Figure 1 allows a *controlled* separation of the center plate from its edges without causing the entire flier plate to fragment. A plastic sheet wrapped around the circumference of the flier plate provides sufficient friction to hold it in position in the target fixture section of the barrel extension.

2.3 Projectile Design

A lexan projectile which has a facing of a graded-density material "pillow" backed by either copper or tantalum is used in these studies. A pillow is fabricated using powder metallurgical techniques such that a smooth variation in its shock impedance occurs through its thickness. The shock impedance of the impact surface of the graded-density material is that of polyolefin, and the shock impedance of the back surface of the pillow resembles copper. When this graded-density material is used to impact a titanium alloy flier-plate at a velocity of ~ 6.4 km/s, an initial shock of approximately 50 GPa, followed by a ramp wave to 100 GPa is introduced into the flier plate. The tantalum backing to the pillow provides higher peak stresses upon impact which can result even higher velocities for the flier plate. The diameter of the pillow facing and its copper or tantalum backing used in this study was ~ 27 mm.

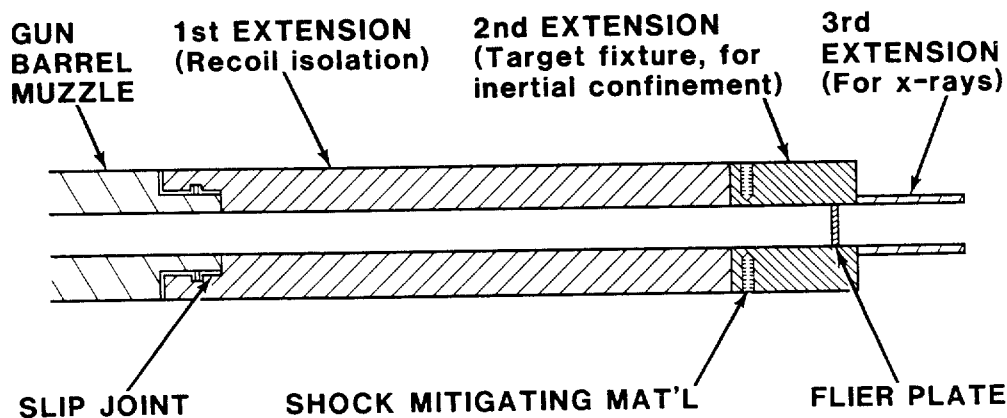


Figure 2. The three barrel extensions used to modify the current two-stage light-gas gun.

Table I: Summary of Experiments

Shot No.	Pillow Thickness (mm)	Backing Material	Backing Thickness (mm)	FlierPlate Material	FlierPlate Thickness (mm)	Buffer Thickness (mm)	FlierPlate Velocity (km/s)
Ti38	2.020	Copper	2.055	Ti-6Al-4V	1.030		9.0
Ti40	2.206	Copper	2.000	Ti-6Al-4V	2.050		8.1
Ti44	2.206	Tantalum	1.000	Ti-6Al-4V	1.000		9.3
Ti45	2.222	Tantalum	0.996	Ti-6Al-4V	1.002	1.475 ^a	9.5
Ti46	1.9139	Tantalum	0.950	6061-T6 Al	0.983	1.558 ^a	10.4

^a A lexan buffer was used in this experiment.

2.4 Diagnostics

Following impact, seven flash X-rays are taken of the flier plate while it is in motion. They are used to estimate the velocity of the flier plate and also to check for its integrity following impact and subsequent acceleration by the shockless pressure pulse. Four of these flash X-rays are taken while the flier plate is in the aluminum barrel extension, usually a few microseconds after impact. The energy of the first four X-rays is 600 keV, and the pulse duration is ~ 3 ns. The pulse duration is sufficiently small to “freeze” the motion at the present velocities. The other 3 X-rays are taken while the flier plate has exited from the muzzle and are located approximately 80 mm, 170 mm, and 350 mm from the impact position. These X-rays sources have a 300-450 keV energy and a 25 ns pulse duration. Due to the hypervelocities achieved in this study, the 25 ns pulse duration can cause a 250 μm blurring of the flier plate while in flight. Radiographic pictures of the flier plate taken in flight over these large distances allow an accurate measurement of its velocity. The flier plate velocity is determined to within $\pm 1\%$ and is listed in Table I.

3 RESULTS

Table I summarizes the impact conditions and the results of the present series of experiments. A titanium alloy was used in this study for the flier plate material, because of its high-fracture resistance property [6,7]. In all the experiments except Ti44 the projectile impacted the flier plate (or buffer-flier plate combination) at ~ 6.4 km/s. These impact velocities are not measured but are estimates based on the gun performance data and are accurate to $\sim 2\%$. In an attempt to obtain higher flier-plate velocities, the copper backing material of the pillow was replaced by tantalum, and the projectile was made to impact the titanium alloy flier plate at ~ 6.9 km/s in experiment Ti44. Lexan buffers were used in experiments Ti45 and Ti46 in an attempt to further cushion the launch. The lexan buffer also reduces the magnitude of the tensile states generated in the flier plate material as a result of wave interactions. This has allowed the launching of a 6061-T6

aluminum alloy plate to 10.4 km/s because the tensile states formed in the flier plate did not exceed the spall strength. Radiographs of all the experiments are shown in Figures 3 to 7. Details of each experiment are presented as an extended figure caption.

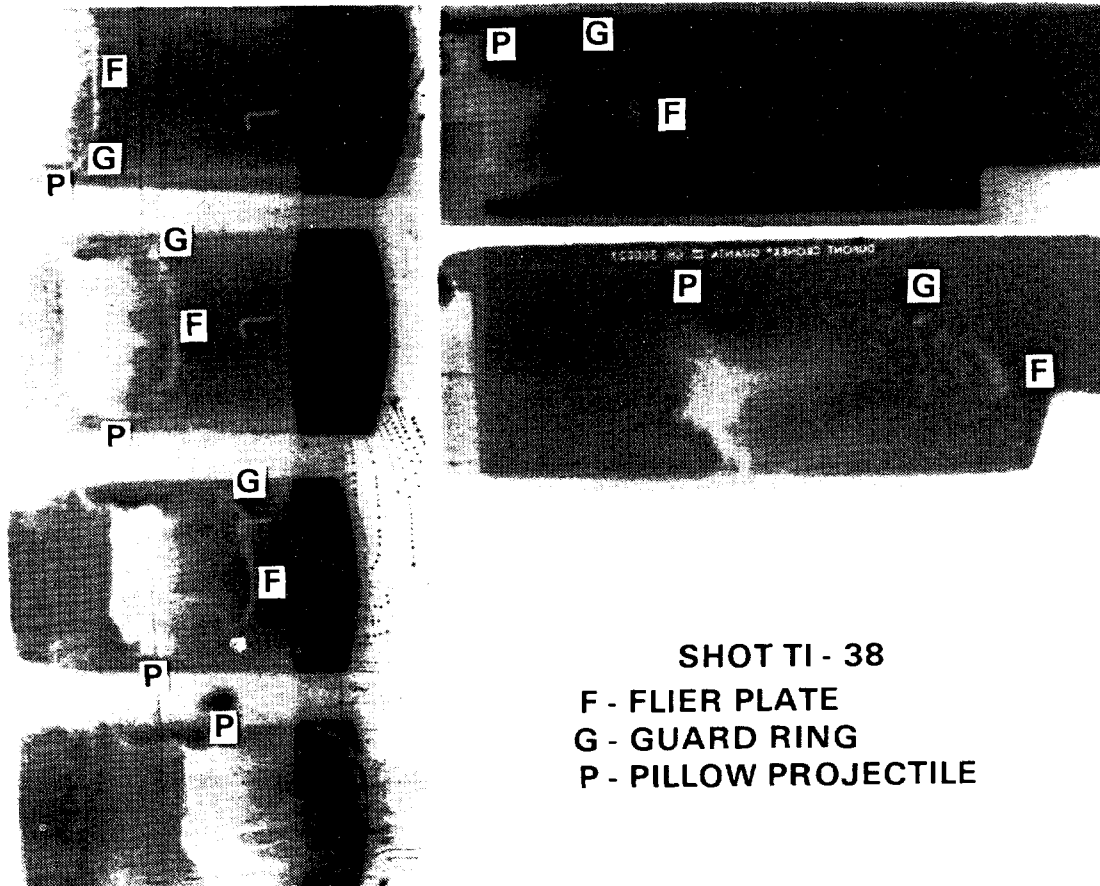


Figure 3. X-ray radiographs of experiment Ti38. The flier-plate is moving (from left to right) at a velocity of 9.0 km/s in this experiment. Top left (Frame 1) shows the flier-plate exiting the tungsten target fixture as it enters the aluminum barrel extension. The sequence of radiographs indicated on the left is taken over a flight distance of 58 mm. The radiographs on the right are taken after exit from the muzzle, after a travel distance of 80 mm and 156 mm from impact, respectively. Although the flier-plate is relatively flat and intact in the first four radiographs, it appears to have folded onto itself after a propagation distance of 156 mm. The remnants of the pillow after impact are seen to be trailing the flier plate at a velocity of ~ 4.5 km/s. The center plate mass is 1.3 gms.

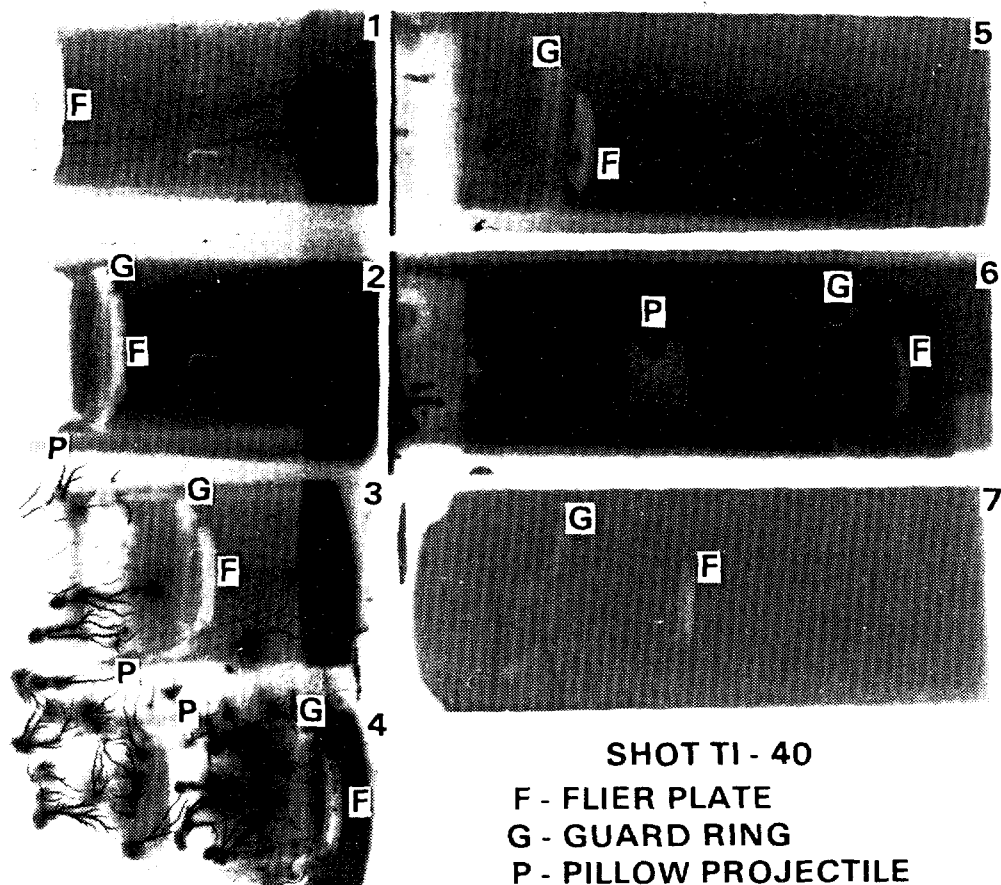


Figure 4. Radiographs of experiment Ti40. The flier-plate is moving from left to right at a velocity of 8.1 km/s. The sequence of radiographs indicated on the left are taken over the first 60 mm from launch impact position. The radiographs on the right is taken after exit from the aluminum muzzle after a travel distance of 85 mm, 152 mm and 357 mm from impact, respectively. As indicated in the figure, the flier-plate is extremely flat even after a propagation distance of 357 mm. This is believed to be due to a variety of optimal experimental impact conditions, such as a) extremely good impact with very little impact misalignment (tilt), b) a good (uniform) pillow, and c) the thicker flier-plate dimension in this experiment. This is evidenced by the symmetry of the projectile/pillow debris trailing the flier plate at a velocity of ~ 5.5 km/s. The mass of the center plate is 2.6 gm.

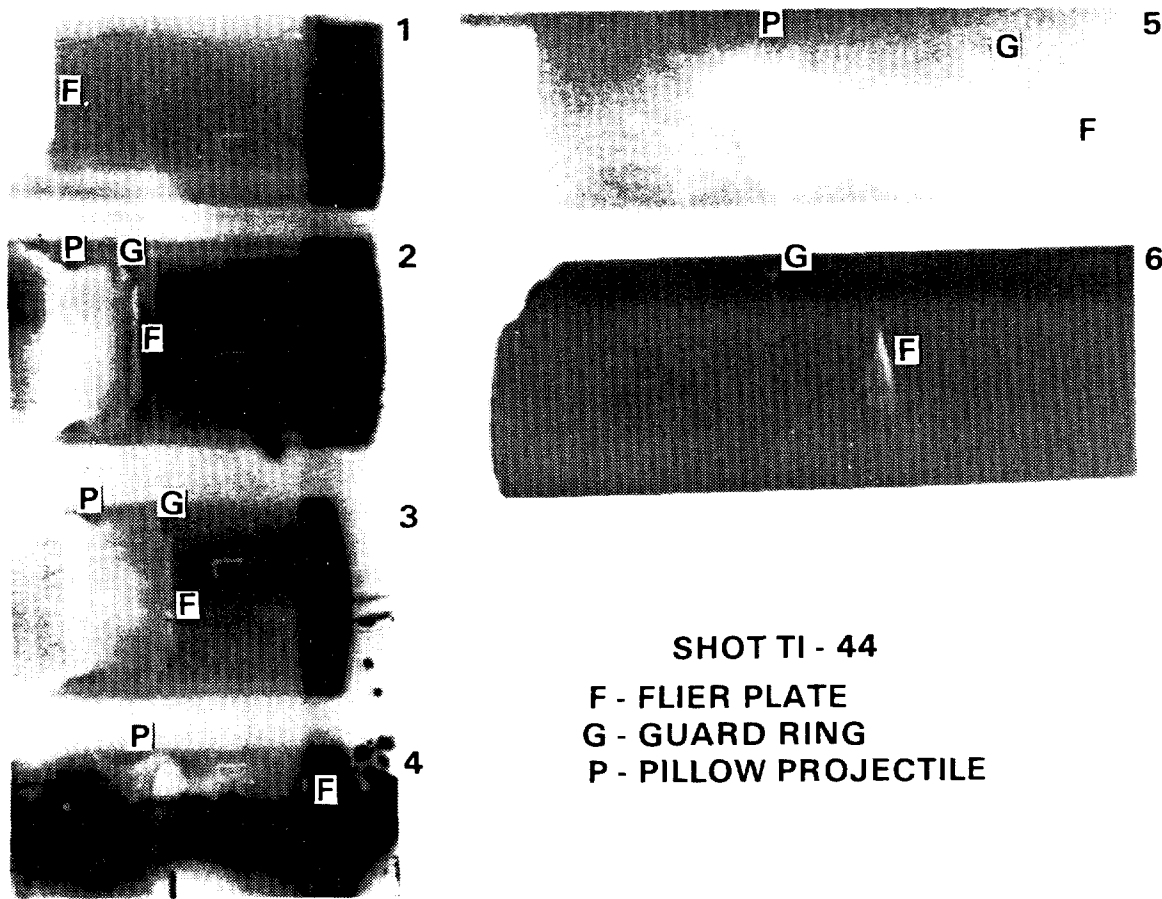


Figure 5. Radiographs of experiment Ti44. The flier-plate is moving from left to right at a velocity of 9.3 km/s. Faster flier-plate velocity is achieved in this experiment both because the pillow is backed by tantalum (to generate higher loading pressures), and because impact occurs at a higher velocity (6.9 km/s). The sequence of radiographs indicated on the left is taken over the first 60 mm. The radiographs indicated on the right are taken after exit from the muzzle, after a travel distance of 157 mm and 350 mm, respectively, from launch impact, suggesting an intact plate over the duration of the experiment. The projectile debris is travelling at a velocity of ~ 5.3 km/s. The mass of the center plate is 1.3 gm.

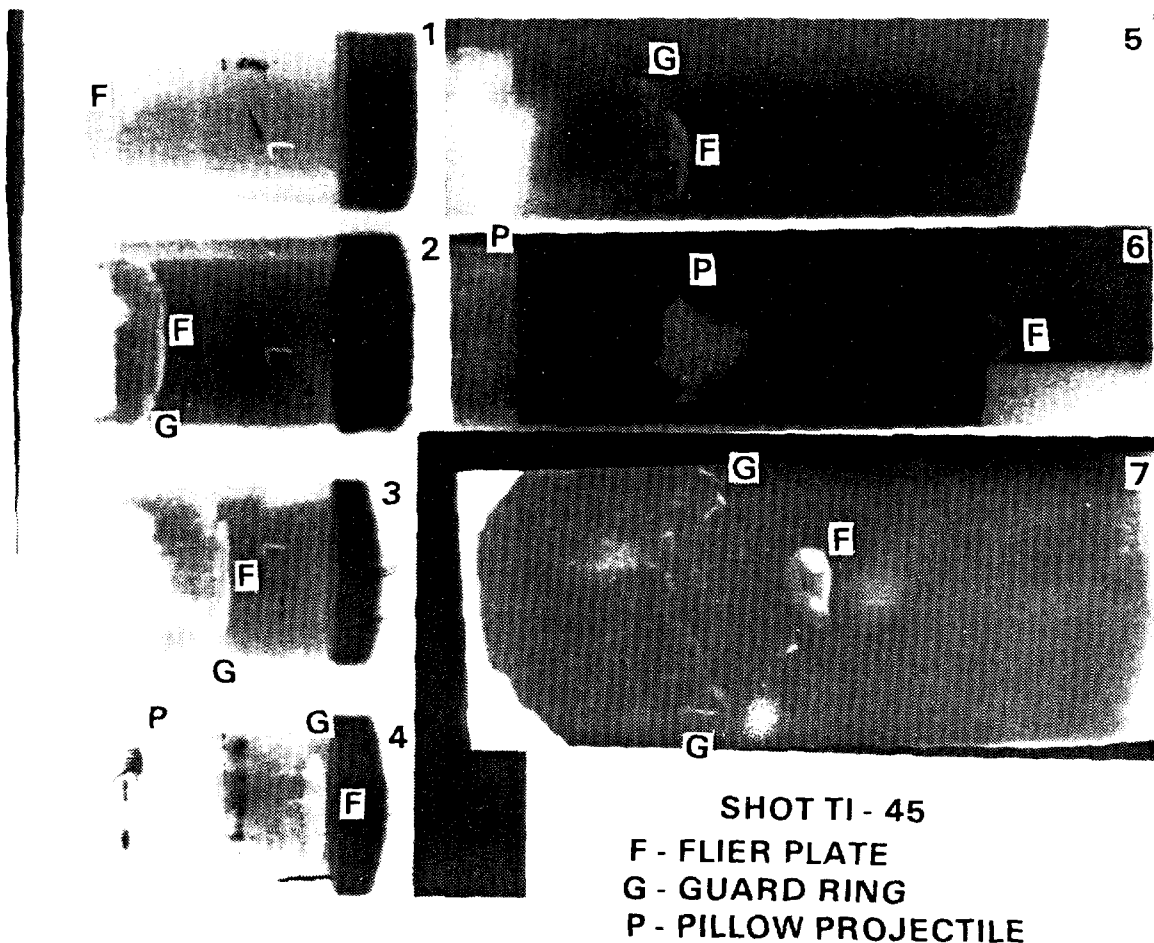


Figure 6. Radiographs of experiment Ti45. In this experiment a lezan buffer was used in an attempt to boost the velocity of the flier-plate. (See section 3.3.) The flier-plate is moving at a velocity of 9.5 km/s, and not at 10 km/s which was anticipated based on calculations. The sequence of radiographs indicated on the left is taken over the first 55 mm from impact. The radiographs on the right are taken after exit from the muzzle, after a travel distance of 84 mm, 156 mm and 345 mm, respectively, from impact. Although the flier plate is relatively flat in the radiographs on the left as it exits the muzzle, it appears to "bow" as it travels further. This may be attributed to significant edge effects in this experiment; due to the presence of a lezan buffer the loading time is increased. A smaller diameter of the central region of the flier-plate is expected to stay relatively flat in similar experiments.

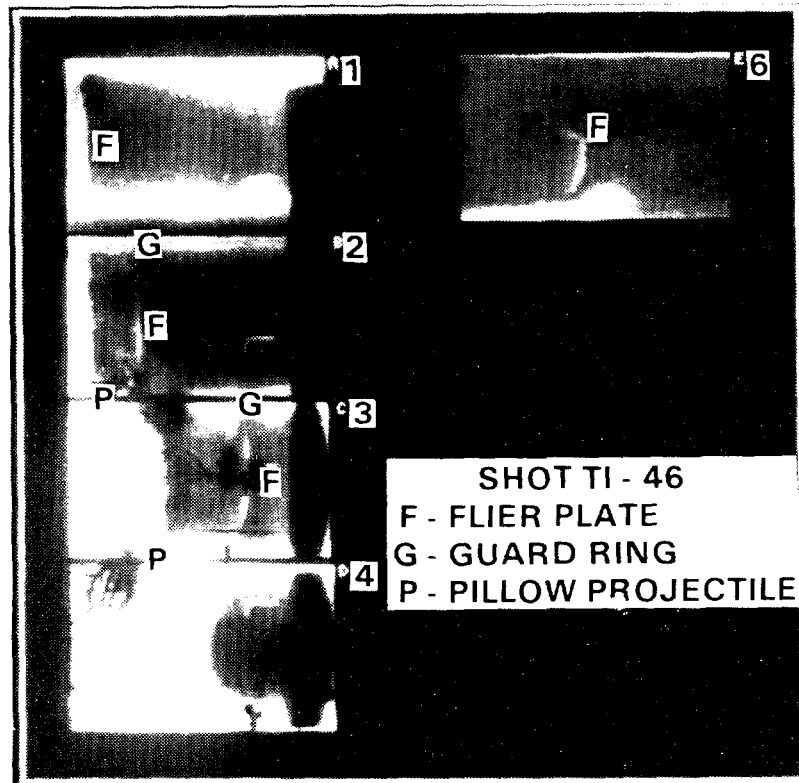


Figure 7. Radiographs of experiment Ti46 showing an aluminum flier plate moving at a velocity of 10.4 km/s. Calculated velocity was also 10.4 km/s. A lezan buffer was used in this experiment. Top left shows the flier-plate exiting the tungsten target fixture after launch impact while in the aluminum barrel extension. The sequence of radiographs indicated on the left is taken over the first 60 mm. The radiograph on the top right is taken after exit from the muzzle, after a travel distance of 170 mm from impact. The flier-plate appears to be flat in the radiographs on the left suggesting a good impact, but increased edge effects due to the presence of a lezan buffer seem to "bow" the plate after further travel. Although not indicated in the above figure the flier plate seems to be intact at a propagation distance of 350 mm. The mass of the center plate is 0.75 gm.

3.1 One-Dimensional Numerical Simulation

Numerical simulations of the pillow impact experiments were made using a version of the Lagrangian code WONDY which uses a tabular equation-of-state (EOS) option [13]. The calculational model treated the pillow as a series of zones having impedances that increase from that of a polymer approximating polyolefin at the impact surface, to that of the copper or tantalum backing plate. The zone thicknesses were chosen so that the impact generates a sequence of multiple shocks in the target; both experiments and calculations have shown that a calculational model of this type gives a loading history that closely approximates the smooth isentropic loading of a pillow [10,12].

For most of the materials in the calculations, the constitutive models used standard Mie-Grüneisen EOS and elastic-perfectly plastic parameters. Further, tensile failure was treated using a maximum principal stress criterion. For the velocity enhancement studies described in Sec. 3.3 tabular EOS were constructed for PMMA and for RDX explosive using the theoretical chemical equilibrium model described in Refs. [14] and [15]. (For calculations, except for its density, the EOS for polyolefin was assumed to be similar to that of PMMA.) Sesame table 5251 [16] was used for the EOS of hydrogen. Tabular EOS were used for PMMA, RDX, and hydrogen, because these materials go through chemical decomposition with high pressures and therefore cannot be represented by a standard Mie-Grüneisen form. The WONDY setups were similar to that for test problem 2 of Ref. [13].

Figure 8 shows some calculated results for shot Ti38 in which the target was a 1 mm thick titanium alloy. The stress history on the base of the target, Fig. 8a, shows an initial shock pressure of about 45 GPa. Although the pressures subsequently exceed 110 GPa, the time-dependent loading conditions keep the temperature well below the melting point. For the titanium alloy flier plate the temperature estimates are approximately one-third its melting point. The calculated stress history at the center of the target, Fig. 8b, suggests that the tensile stresses do not exceed the fracture strength of the titanium alloy, -5.5 GPa [6,7]. (The spall strength measurements were made on the material which was precompressed to ~ 14 GPa. The temperature of the material precompressed to 14 GPa is expected to be much lower than those attained in the present flier plate experiment.) This result agrees with the experimental observation that the plate did not fracture. The velocity history of the base of the target, Fig. 8c, shows a terminal velocity of 9 km/s, in excellent agreement with the measured value (see Table I).

3.2 Two-Dimensional Simulations

As discussed in the previous sections, when a graded-density impactor is used to impact a flier plate, the resultant flier-plate velocity is increased by as much as 60%. As a variation of this technique, variable impedance materials have been used as an intermediate staging arrangement to enhance the target (flier-plate) velocity [17]. The loading on the flier-plate has to be shockless so that the temperature rise in the flier-plate is minimized

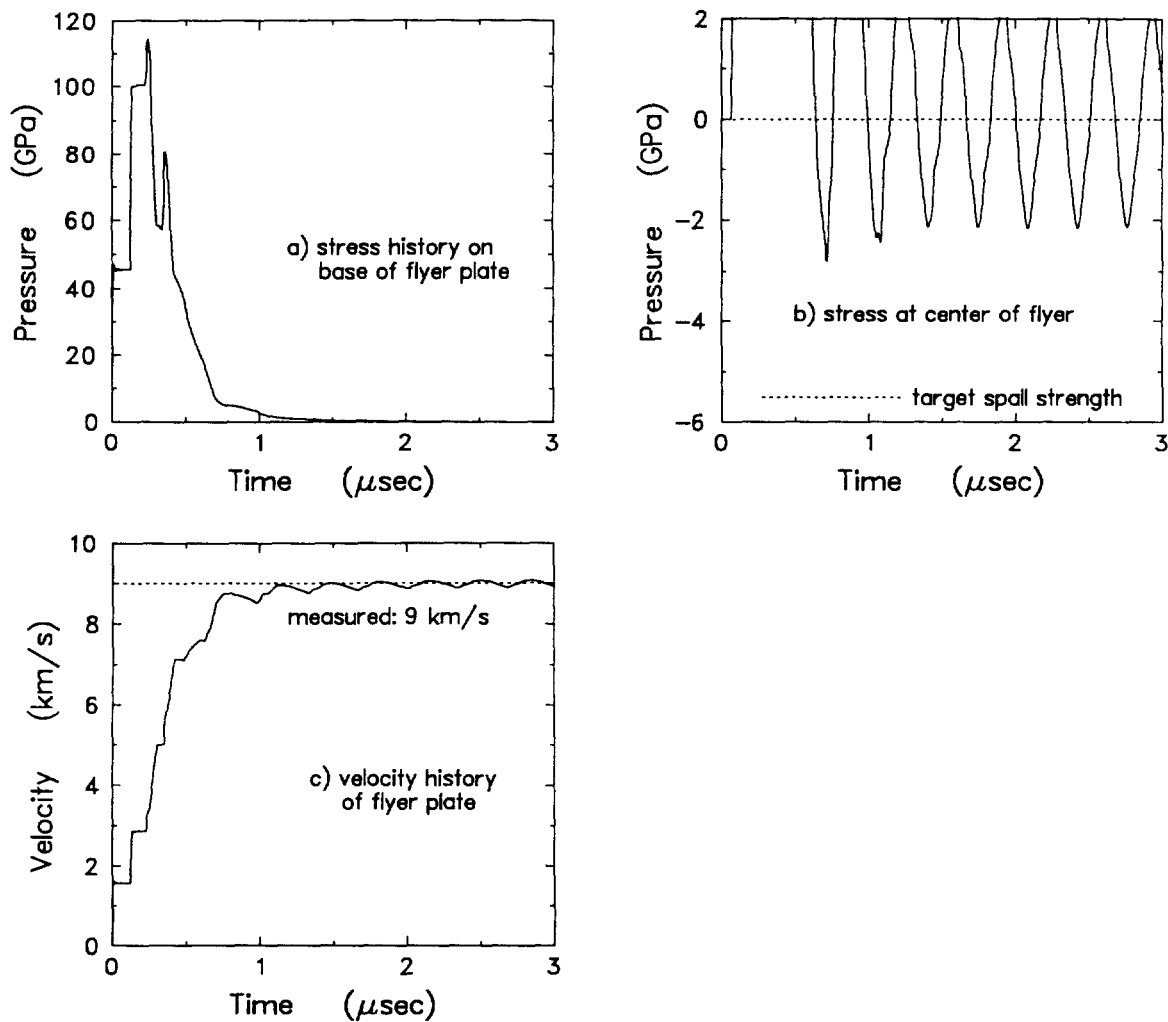


Figure 8. Calculated stress and velocity histories for the flier plate in Shot Ti38.

to prevent the flier-plate from melting. Also, the pressure-pulse has to be tailored sufficiently to prevent spall fracture of the plate resulting from wave interactions. In addition, the flier plate must be laterally confined to minimize two-dimensional effects.

The success of the current approach is partially due to the control of disruptive edge effects by means of radial confinement of the variable impedance impact event at the time of greatest acceleration of the flier. The observed shapes of the flier seen in the radiographs of the experiments reveal the presence/results of edge effects following peak acceleration. Successfully launched fliers are flat, except for regions quite close to their outer radii, where some flier material is bent. In some unsuccessful launches, in which the

flier fragments catastrophically, the flier plate has also shown larger amounts of bending. As indicated in this section, bending of the flier plate is more pronounced when there is poor radial confinement of the impact event. This, then, allows the lower impedance (lexan) part of the gun projectile to jet radially, resulting in inhomogeneous relief of the flier, with consequent heterogeneous stress distributions within the flier. Such a phenomenon then produces large bending stresses within the flier, often extending into the core region. Bending stresses can produce large strain fractures in the flier, providing a secondary mechanism for flier fragmentation, in addition to high strain rate wave-interaction processes.

By performing two dimensional, axisymmetric simulations of key aspects of the experiments we have acquired broad understanding of the significance of radial confinement. While the radiography is quite helpful in revealing bending and disruption of the flier plate, there is no direct experimental probe of the impact region during the times of peak accelerations. Computer simulations can be used to develop qualitative understanding of this region. We have used the Eulerian hydrodynamics code CTH [18] to study the effect of radial confinement. We have used the same approach as discussed in the 1-D calculations, except for the presence of the additional radial degree of freedom. CTH allows all materials in the problem to be modeled as elastic-perfectly plastic solids with a simple critical pressure criterion. The lexan body of the gas-gun projectile is not included in these calculations, however.

We have performed three distinct simulations. In the first, the outer diameter of the gas-gun projectile and titanium alloy flier are confined by the tungsten alloy barrel extension fixture actually utilized in the experiments. In Figure 9 we present a series of four "snapshots" from the calculation, showing the evolution of the impact region at the times of 0, 1, 2, and 3 μsec . A small amount of radial jetting of the lower impedance layers in the projectile occurs upon impact. It is impossible to completely prevent this from happening. But, the tungsten alloy is quite effective in reducing the extent of this jetting. This is seen in the 1 μsec picture, which shows only a small residual deformation of the tungsten fixture. Still, slight bending of the titanium is clearly visible. It is our claim that this bending would be significantly greater in the absence of radial confinement. By the time of 3 μsec , the projectile has generally disintegrated, while the flier remains intact, with a flat central core.

In Figure 10, we show the same time sequence, but in the absence of confinement. At 1 μsec , the jets of low-impedance material are clearly present, with subsequently greater bending of the flier. The central core of the flier still remains quite flat in appearance. The flier looks intact in these pictures, but it should be emphasized that there is no accurate mechanism in the CTH code to predict fracture in highly bent or stretched material. Our experience allows us to view the hydrocode results as conservative predictors of experimental behavior. Therefore, we expect to see greater amounts of fracture experimentally in the unconfined case. The same type of remark provides some explanation for why the break-up of the projectile during the impact does not look completely realistic in these computer plots.

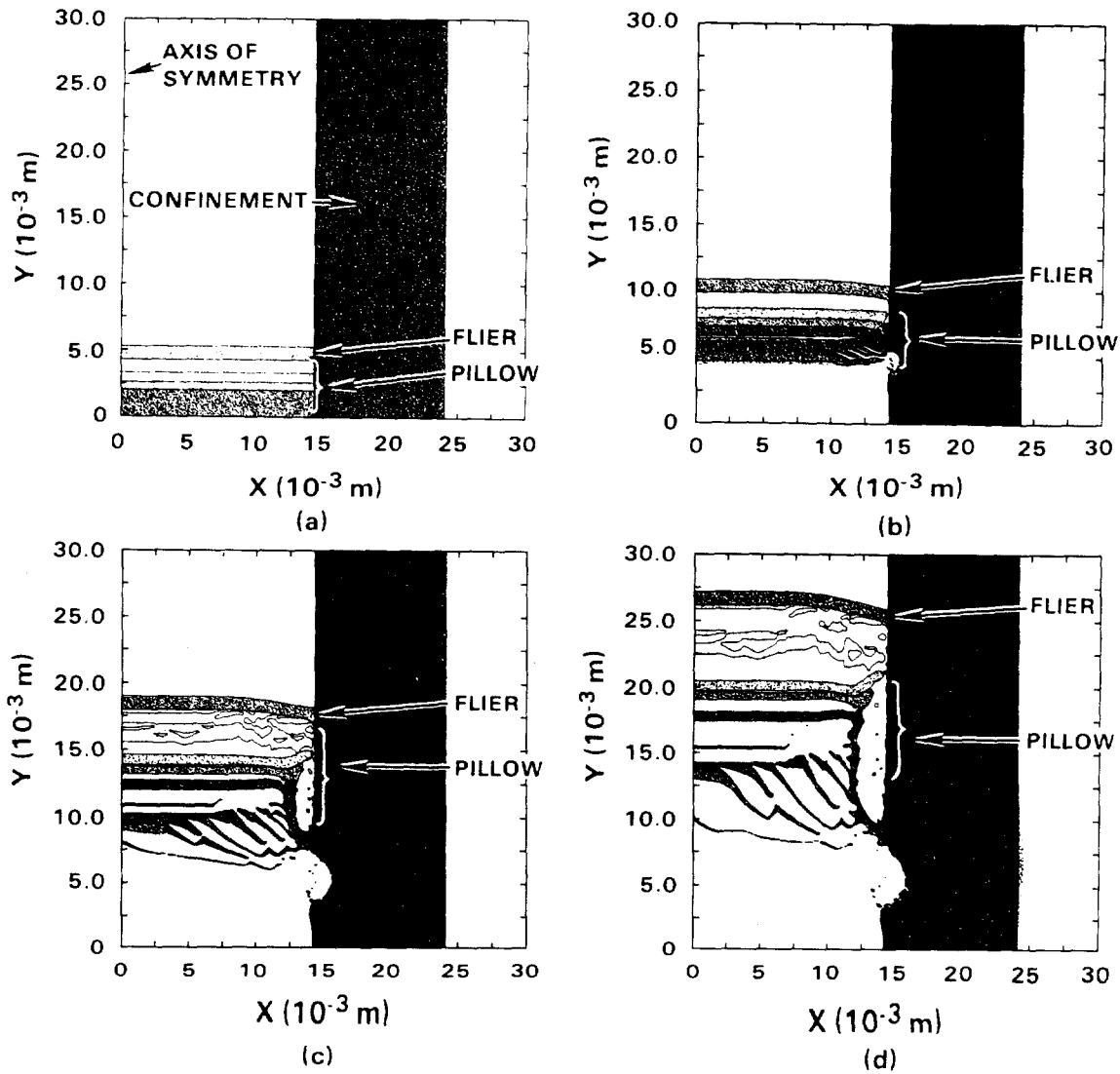


Figure 9. Evolution of pillow impact with tungsten confinement. Times shown are (a) $0.0 \mu\text{sec}$, (b) $1.0 \mu\text{sec}$, (c) $2.0 \mu\text{sec}$, and (d) $3.0 \mu\text{sec}$.

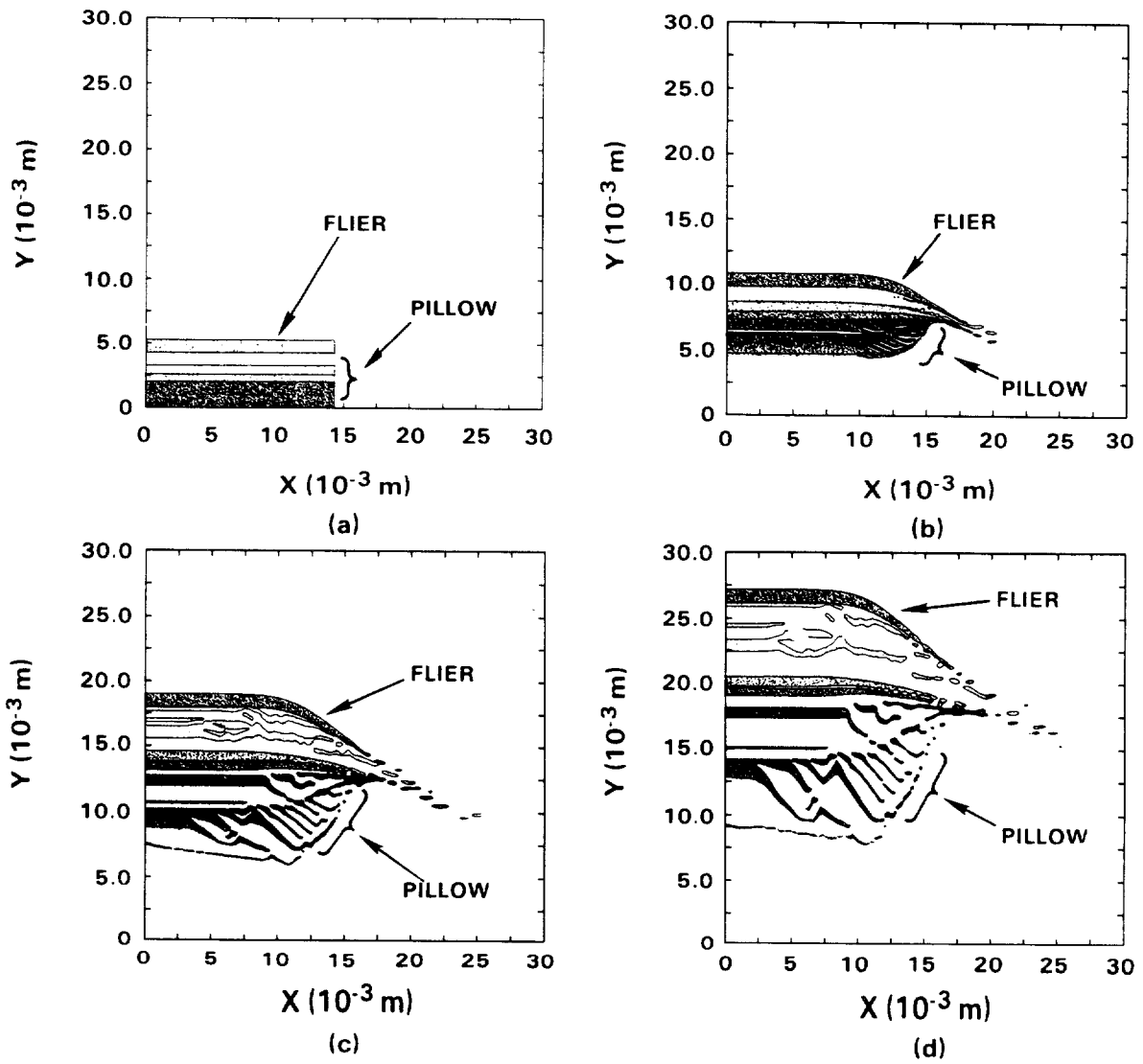


Figure 10. Evolution of pillow impact with no confinement. Times shown are (a) $0.0 \mu\text{sec}$, (b) $1.0 \mu\text{sec}$, (c) $2.0 \mu\text{sec}$, and (d) $3.0 \mu\text{sec}$.

Confinement is desirable for maximizing the diameter of intact flier. It may not be essential for launching the core region of the flier, however. But, this core region must then be isolated, using guard-rings or something similar, from the edge interactions. This not only prevents wave-propagation induced fractures from propagating in from the outer radius, but it also allows the intact core of the flier to “pop” free as the flier plate bends during launch and flight.

In certain applications, a small diameter, intact core may not be sufficient, and so confinement certainly would be desired. An engineering issue, then, is whether a less expensive material than tungsten alloy can be used as a confining barrel extension in these experiments. For this reason, we performed one calculation using steel as the confining fixture. Figure 11 shows the evolution of the resulting impact. Calculationally, a slightly greater amount of bending takes place. The steel was less effective at resisting the initial jetting, as shown by the larger area of the deformed region in the fixture.

We can quantify these results somewhat. In Figure 12 we compare the configuration of the flier between the tungsten confined and unconfined case. Also overlaid in these plots are contours of tensile pressure. The greatest tensile states at 3.0 μ sec has increased from between -0.7 GPa and -0.8 GPa to between -0.8 GPa and -0.9 GPa. In Figure 13 we make the same comparison between the tungsten confined and steel confined fliers. The greatest tensile states has not increased in this case. However, while isolated regions of tensile stress between -0.7 GPa and -0.8 GPa were present with tungsten confinement, in the case of steel confinement the entire central region of the flier is subjected to this increased level of tensile stress.

Tensile states do not directly reflect the bending strain of the flier. In Figure 14 we plot σ_{xy} bending stress as a function of time at a location in the middle of the flier plate, and at a radius of 1.0 cm, for all three of these calculations. This figure displays the trends that we have just discussed. The presence of wave reverberations within the flier is clearly seen in this figure. Note that the peak levels of the bending stress increases as we proceed from tungsten confinement, to steel confinement, and finally to no confinement. By 3.0 μ sec, the bending stress level in the unconfined case is very different from that associated with either of the two types of confinement. We have not performed experiments with steel fixtures yet, but it seems likely that they will be successful in launching intact fliers.

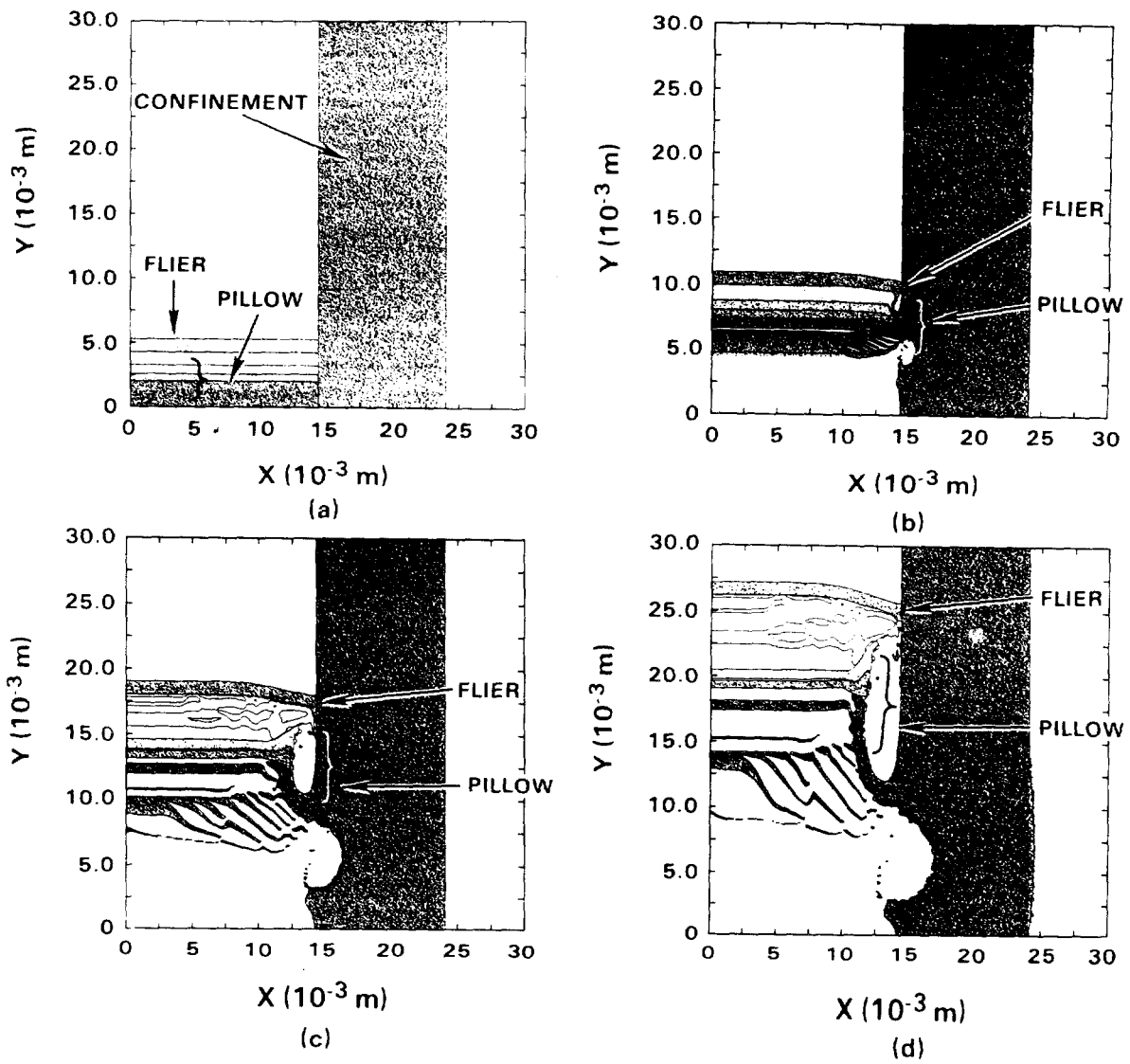
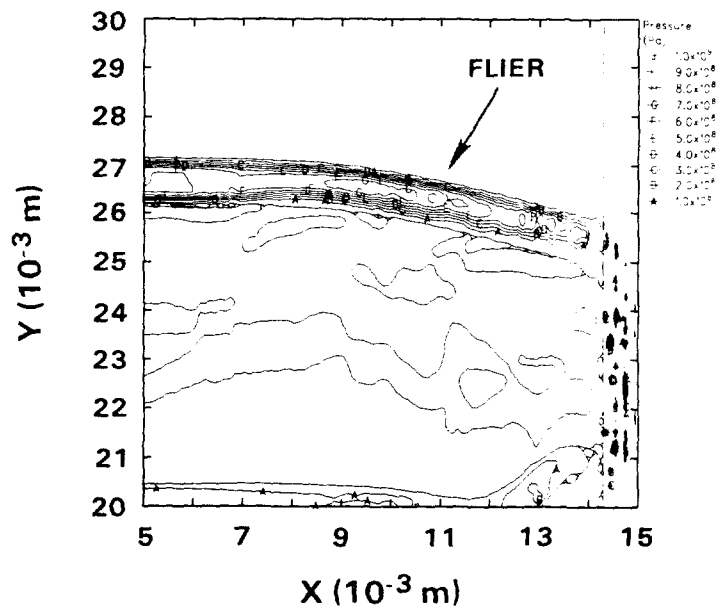
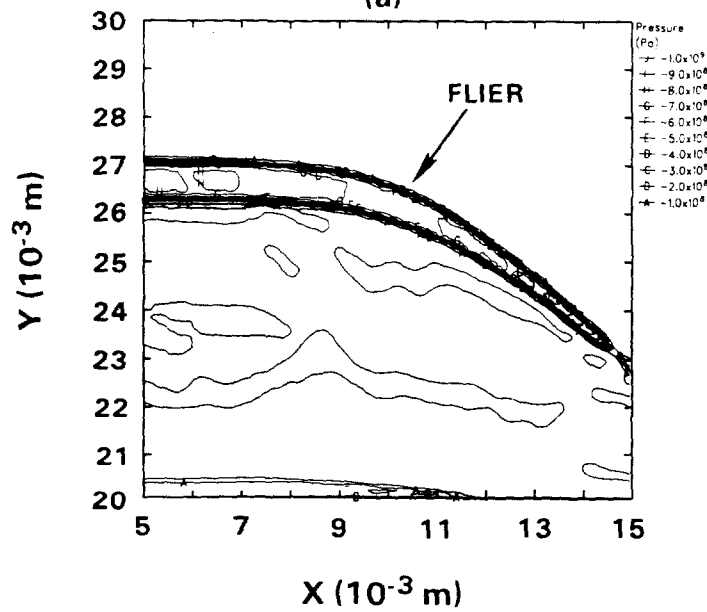


Figure 11. Evolution of pillow impact with steel confinement. Times shown are (a) 0.0 μsec , (b) 1.0 μsec , (c) 2.0 μsec , and (d) 3.0 μsec .



(a)



(b)

Figure 12. Comparison of (a) tungsten confined and (b) unconfined flier plate at 3.0 μ sec. Tensile stress contours are shown.

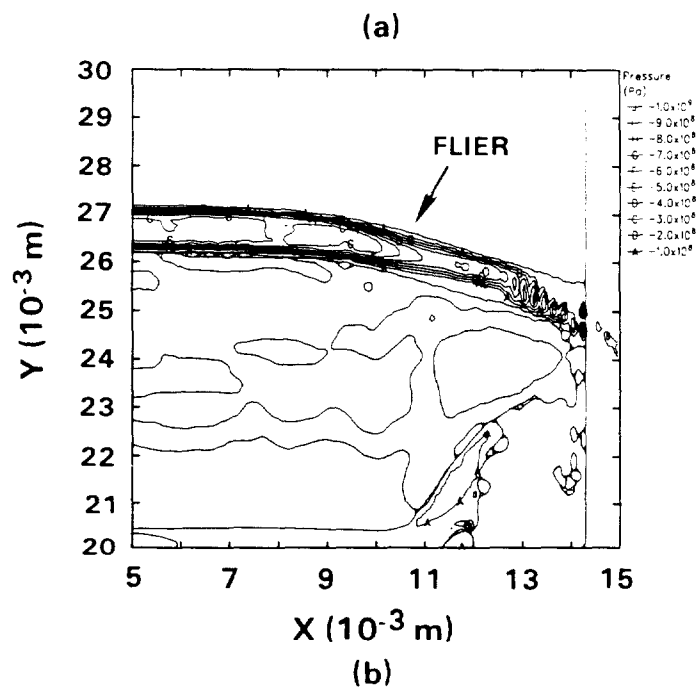
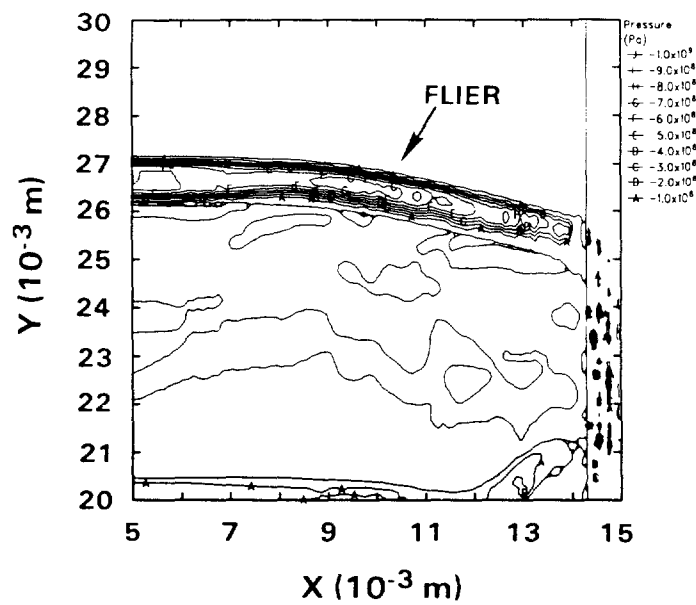


Figure 13. Comparison of (a) tungsten confined and (b) steel confined flier plate at 3.0 μsec. Tensile stress contours are shown.

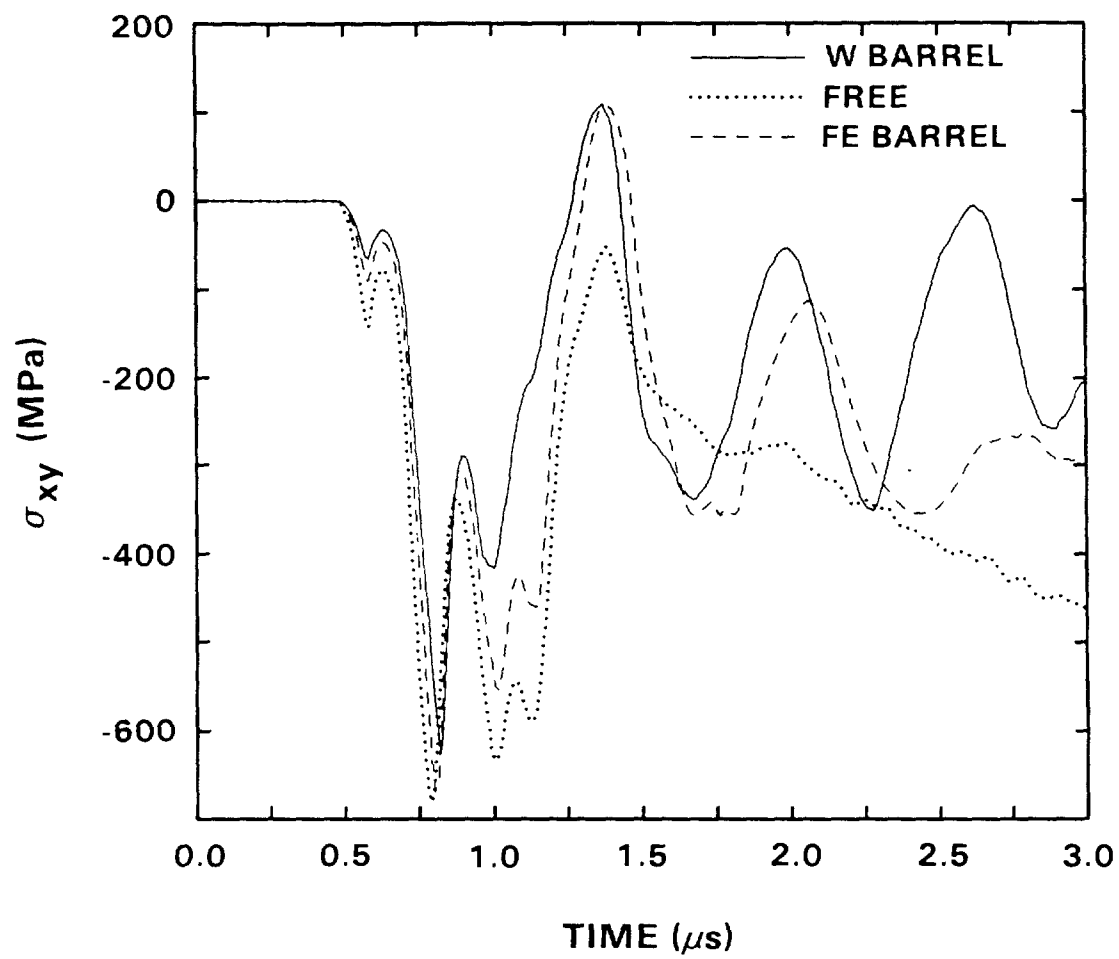


Figure 14. Plot of σ_{xy} vs time in the fier plate at a radius of 1.0 cm.

3.3 Velocity Enhancement

Studies in the present program have also focused on exploring methods to achieve even higher plate velocities. Some of the possible velocity enhancement methods are discussed in this section. Studies using the WONDY code show that increased flier velocities could be obtained using buffer layers of plastic, explosive, or hydrogen on the impact surface. Calculations have indicated, that as a result of high-pressure compression and decompression these materials behave “energetically” in that the expansion velocities of these materials are extremely high. This results in an efficient “push” on the flier and can further enhance its velocity.

An examination of the results shown in Fig. 8 suggested that adding plastic on the pillow surface not only cushions the impact, but that expansion of this layer at late times adds an extra push that increases the terminal velocity. Specifically, a WONDY calculation predicted that the addition of a 2 mm plastic layer on the impact surface of the target plate would increase the terminal velocity (of the experiment Ti38; calculational results shown in Figure 8) from 9.0 to 9.7 km/s. A similar calculation, but with 2 mm of RDX explosive instead of plastic, predicted a final velocity of 10.25 km/s. Additional calculations gave the following results:

- The velocity increase is roughly proportional to the thickness of the buffer layer up to a thickness of at least 2 mm.
- Higher velocities are obtained when the buffer layer is placed on the impact surface of the target rather than on the front of the impactor.
- Adding layers to *both* the impactor and the target enables one to tailor the loading history and to minimize both the initial impulse and the tensile states produced in the target.
- Lowering the density of the buffer material results in a softer impulse on the flier without decreasing the terminal velocity.

Two experiments were carried out to test the calculational predictions. For shot Ti45, which had a 1.5 mm plastic buffer and an impactor backed with tantalum, WONDY predicted a terminal velocity of 10.0 km/s. In the experiment the measured value was 9.5 km/s. For shot Ti46, in which the flier plate was aluminum instead of titanium, the predicted velocity was 10.4 km/s, in excellent agreement with the experimental result. Calculated stress and velocity histories for shot Ti46 are shown in Figure 15. Comparing with Figure 8, it can be seen that the buffer layer substantially reduces both the initial impulse and the tensile stresses. Hence the plastic not only enhances the velocity of the flier but also reduces its tendency to melt or to fracture.

Because of the softer loading history produced with a buffer layer, a computational study was made to see if the same system could be used to launch flier plates made of

other materials. WONDY calculations were made for the same configuration as shot Ti46, except with 1-gm target plates of tantalum, molybdenum, iron, and a tungsten alloy. In all four cases, a terminal velocity of over 10 km/s was predicted without either melting or fracture.

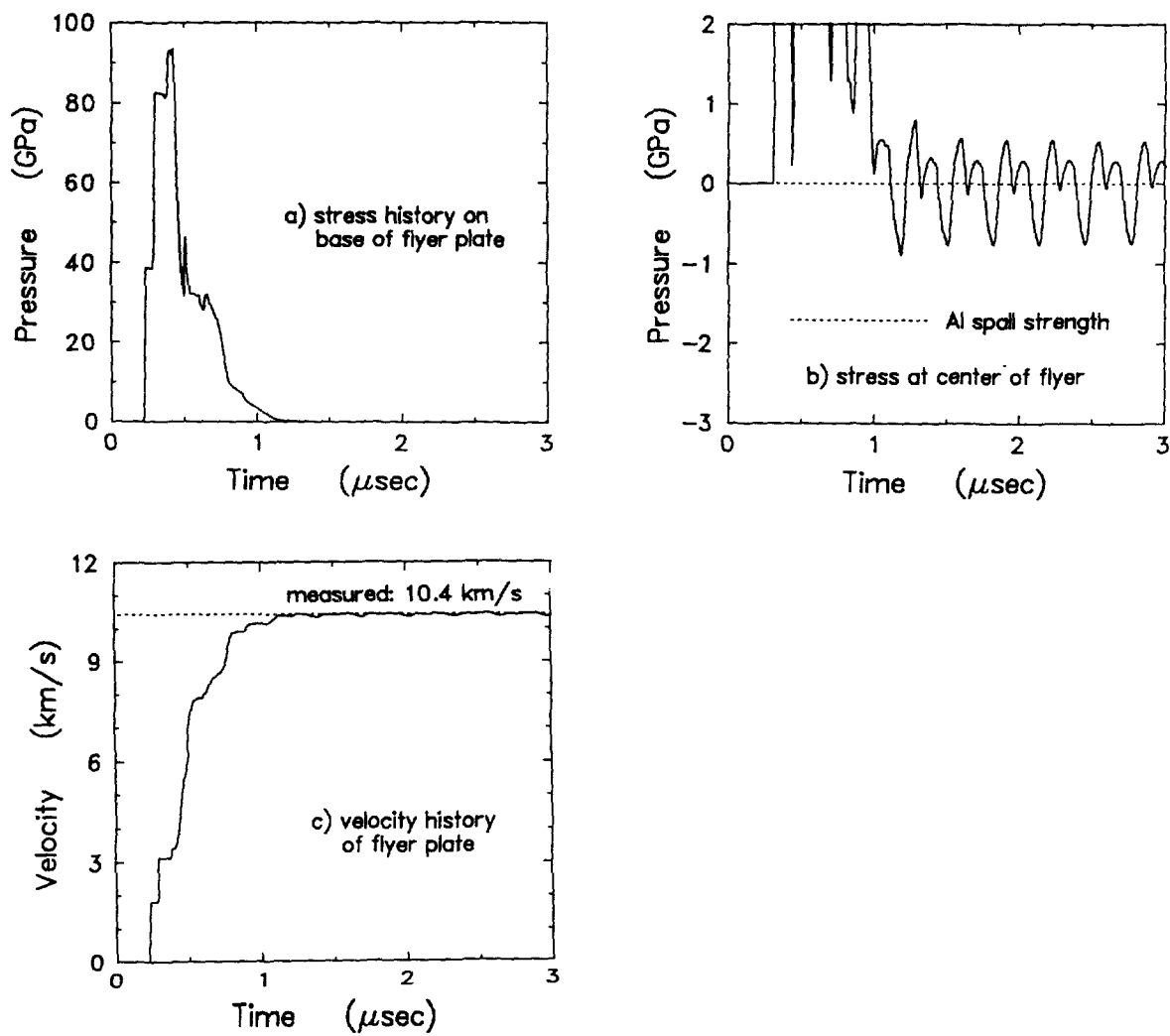


Figure 15. Calculated stress and velocity histories for the flyer plate in Shot Ti46.

Additional studies were made to see if hydrogen, with its high sound speed, could be used to further enhance flier velocities. By replacing the plastic buffer in shot Ti46 with a 10-mm layer of liquid H_2 , the velocity was predicted to increase from 10.4 km/s to 11.3 km/s. Figure 16 shows the stress and velocity histories for a similar computational experiment, in which the impactor velocity was increased to 8.0 km/s. In this case, it proved necessary to add a thin plastic layer to the front of the impactor in order to eliminate fracture. The calculation predicts a final velocity of 14.0 km/s for this design, even though the loading is much softer than what was obtained in shot Ti46. Hence hydrogen buffers appear to offer a way to achieve the extremely high flier velocities.

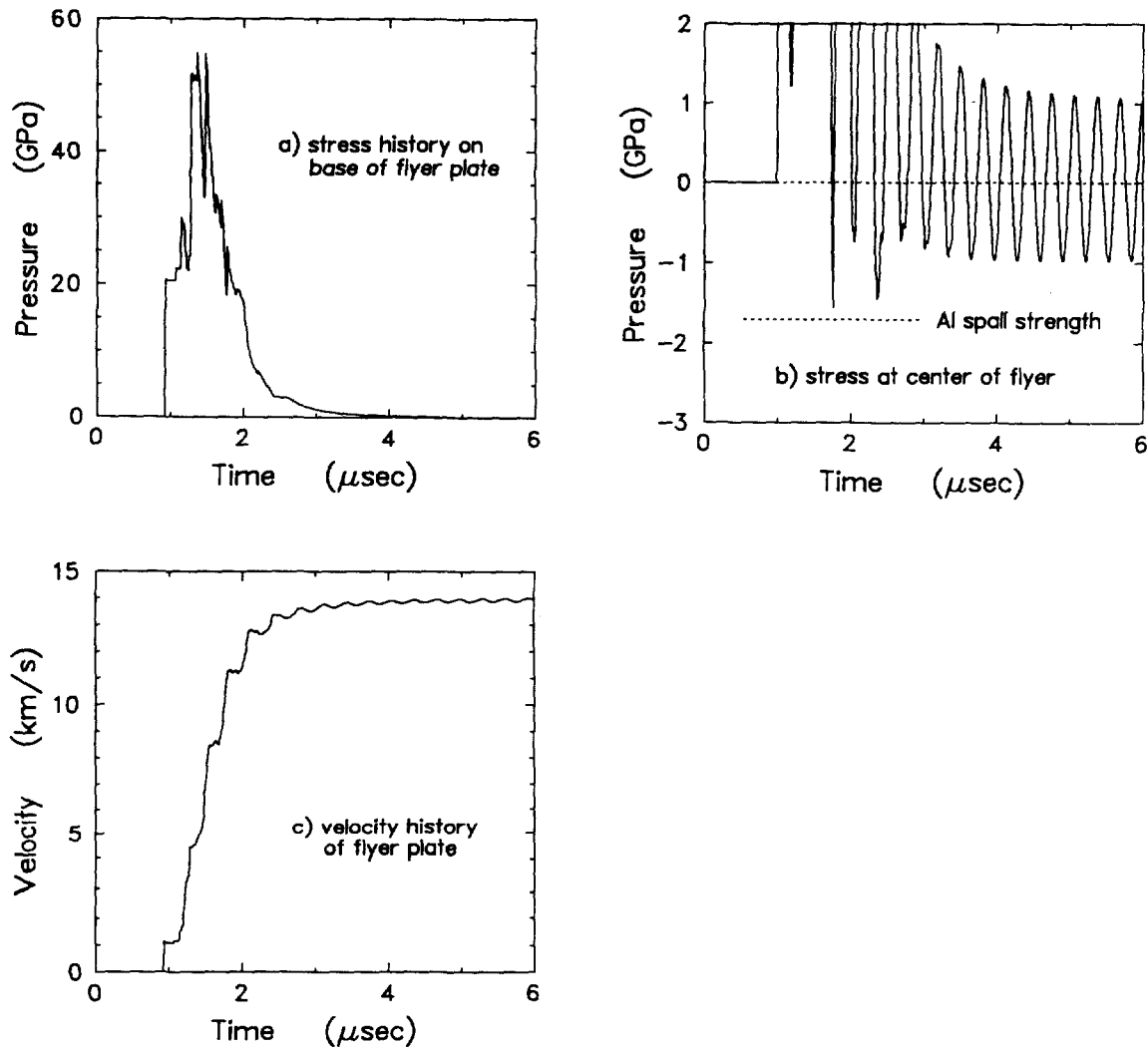


Figure 16. Calculated stress and velocity histories for the flier plate in a hydrogen-buffered experiment.

4 SUMMARY

A systematic study has been described which allows launching of gram-size plates to hypervelocities. In particular, a 0.8 gm, 6061-T6 aluminum flier plate has been launched intact to a velocity of 10.4 km/s. This has been achieved by using a graded-density impactor to impact a flier-plate at a velocity of ~ 6.4 km/s on the two-stage light-gas gun. Upon impact, a shockless *i.e.*, a time-dependent high pressure (100 GPa) pulse is produced at the flier-plate/impact interface. This allows shockless acceleration of the flier-plate to hypervelocities without causing excessive heating leading to melt or vaporization. The pressure pulse must be tailored, however, to prevent spall fracture of the plate. Although the technique has been used currently to launch Ti-6Al-4V alloy and 6061-T6 aluminum alloy plates, calculations suggest that this technique can be extended to include other (high-density) materials.

Confinement is desirable for maximizing the diameter of intact flier. It may not be essential for launching the central region of the flier, however. But, this central region must then be isolated, using guard-rings from the edge interactions. This not only prevents wave-propagation induced fractures from propagating in from the outer radius, but it also allows the intact core of the flier to separate in a controlled fashion as the flier plate bends during launch and flight. Tungsten makes a good confinement fixture, but calculations have indicated that a cheaper material such as steel could be substituted to provide a satisfactory confinement.

The flier plate velocities can be further enhanced either by using explosives, plastics, or hydrogen as a first layer of the graded-density impactor or on the flier plate itself. Calculations have indicated that as a result of high-pressure compression and decompression these materials behave "energetically," in that the expansion velocities of these materials are extremely high. This results in an efficient "push" on the flier plate and can further enhance the flier plate velocity. This concept has been verified by successfully launching a plastic buffered aluminum plate to a record velocity of 10.4 km/s. The buffer has the added advantage in that it can mitigate spall fracture from occurring in the flier plate. Calculations have also suggested that velocities in excess of 12 km/s are possible with a non-buffered flier plate with an increase in the impact velocity to 8 km/s from our current impact velocity of 6.4 km/s. This can be obtained by using a 20 mm bore barrel on the two-stage light-gas gun, instead of the 28 mm bore barrel which was used in these studies.

5 ACKNOWLEDGMENTS

The authors wishes to acknowledge the able and cheerful technical assistance provided by W. Reinhart and J. M. Miller during the course of this investigation.

6 REFERENCES

1. J. R. Asay, L. C. Chhabildas, and L. M. Barker, *Projectile and Impactor Designs for Plate-Impact Experiments*, Sandia Laboratories Report No. SAND85-2009, 1985.
2. R. G. McQueen and S. P. Marsh, *High Explosive Systems for Equation-of-State Studies*, Shock Waves in Condensed Matter 1987, Edited by S. C. Schmidt and N. C. Holmes, Elsevier Science Publishers B. V., 1988, pg. 107.
3. J. R. Asay, T. G. Trucano, and R. S. Hawke, *The Use of Hypervelocity Launchers to Explore Previously Inaccessible States of Matter*, J. Impact Engg., V 10, pg. 51, 1990.
4. L. M. Barker, L. C. Chhabildas, and T. G. Trucano, *High Gas Pressure Acceleration of Flier Plates: Experimental Technique*, J. Impact Engg., V10, pg. 67, 1990.
5. L. M. Barker, L. C. Chhabildas, T. G. Trucano, and J. R. Asay, *Gas Accelerated Plate Stability Study*, in Shock Waves in Condensed Matter - 1989, ed. by S. C. Schmidt, J. N. Johnson, and L. W. Davison, Elsevier Science Publisher, pg. 989, 1990.
6. L. C. Chhabildas, L. M. Barker, J. R. Asay, and T. G. Trucano, *Relationship of Fragment Size to Normalized Spall Strength for Materials*, J. Impact Engg., V10, pg. 107, 1990.
7. L. C. Chhabildas, L. M. Barker, T. G. Trucano, and J. R. Asay, *Spall Strength Measurements on Shock-Loaded Refractory Metals*, in Shock Waves in Condensed Matter - 1989 ed. by S. C. Schmidt, J. N. Johnson, and L. W. Davison, Elsevier Science Publisher, pg. 429, 1990.
8. J. R. Asay, L. C. Chhabildas, G. I. Kerley, and T. G. Trucano, *High Pressure Strength of Shocked Aluminum*, in Shock Waves in Condensed Matter - 1985, ed. by Y. M. Gupta, Plenum Publishers, pg. 145, 1986.
9. R. G. McQueen, J. N. Fritz, and C. E. Morris, in Shock Waves in Condensed Matter - 1983, ed. by J. R. Asay, R. A. Graham, and G. K. Straub, Elsevier Science Publisher, pg. 95, 1984.
10. L. C. Chhabildas, J. R. Asay, and L. M. Barker, *Shear Strength of Tungsten Under Shock- and Quasi-Isentropic Loading to 250 GPa*, Sandia National Laboratories Report No. SAND88-0306, April 1988.
11. L. M. Barker, *High-Pressure Quasi-Isentropic Impact Experiments*, in Shock Waves in Condensed Matter - 1983, ed. by J. R. Asay, R. A. Graham, and G. K. Straub, Elsevier Science Publishers, pg. 217, 1984.

12. L. C. Chhabildas and L. M. Barker, *Dynamic Quasi-Isentropic Compression of Tungsten*, Shock Waves in Condensed Matter 1987, Edited by S. C. Schmidt and N. C. Holmes, Elsevier Science Publishers B. V., 1988, pg. 111.
13. G. I. Kerley, *A Tabular Equation of State Option for the WONDY Code*, Sandia National Laboratories report SAND88-0831, 1988.
14. G. I. Kerley, *Theoretical Equations of State for the Detonation Properties of Explosives*, in Proceedings of the Eighth Symposium (International) on Detonation, edited by J. M. Short (Naval Surface Weapons Center, White Oak, MD, 1986), NSWC MP 86-194, pp. 540-547.
15. G. I. Kerley, *Theoretical Model of Explosive Detonation Products: Tests and Sensitivity Studies*, to be published in Proceedings of the Ninth Symposium (International) on Detonation, Aug. 28 - Sep. 1, 1989, Portland, OR.
16. K. S. Holian, *T-4 Handbook of Material Properties Data Bases*, Los Alamos National Laboratory report LA-10160-MS, 1984.
17. G. R. Fowles, C. Leung, R. Rabie, and J. Shaner, *Acceleration of Flat Plates by Multiple Staging*, in High Pressure Science and Technology, Edited by K. D. Timmerhaus and M. S. Barber, Plenum Press 1979, pg. 911, 1979.
18. J. M. McGlaun, S. L. Thompson, L. N. Kmetyk, and M. G. Elrick, *A Brief Description of the Three-Dimensional Shock Wave Physics Code CTH*, Sandia National Laboratories, SAND89-0607, July, 1990.

DISTRIBUTION

Los Alamos National Laboratory
Mail Station 5000

P.O. Box 1663

Los Alamos, NM 87545

Attention:

B. I. Bennett, T-1, MS B221
S. T. Bennion, X-4, MS F664
P. J. Blewet, X-5, MS F669
T. F. Bott, Q-6, MS K557
B. Daly, T-3, MS B216
N. S. DeMuth, S-3, MS F607
J. Dienes, T-3, MS B216
J. C. Doyle, S-3, MS F607
S. Eisenhower, Q-6, MS K559
P. Follansbee, MST-5, MS G730
J. N. Fritz, M-6, MS J970
R. P. Godwin, X-3, MS F663
J. W. Gordon, X-2, MS B220
F. H. Harlow, T-3, MS B216
W. B. Harvey, X-4, MS F664
J. W. Hopson, X-4, MS F664
J. N. Johnson, T-14, MS B214
N. L. Johnson, T-3, MS B216
M. Klein, X-5, MS F669
L. B. Luck, Q-6, MS K559
S. P. Marsh, M-6, J970
G. H. McCall, X-DO, B218
R. G. McQueen, M-6, J970
J. H. Norman, X-5, MS F669
C. E. Ragan, P-3, D449
T. Sandford, DRA/NDR MS F617
J. W. Shaner, MDO, P915
W. Sparks, X-5, MS 669
R. D. Steele, M-1, C920
T. H. Tan, M-6, J970
J. W. Taylor, DRA/IMA, MS F681
J. D. Wackerle, M-9, P952

Professor T. J. Ahrens
Seismological Laboratory, 252-21
California Institute of Technology
Pasadena, CA 91125

Mr. L. M. Barker
13229 Circulo Largo Ct, N.E.
Albuquerque, NM 87111

Dr. M. J. Bjorkman
Boeing Aerospace and Electronics
P.O.Box 1470
Huntsville, AL 35807-3701

Dr. Jeanne Crews
SN3 - Hypervelocity Impact Laboratory
NASA, Johnson Space Center
Houston, TX 77058

Dr. D. P. Dandekar
Department of the Army
Army Materials and Mechanics
Research Center
Watertown, MA 02171

Washington State University
Department of Physics
Pullman, WA 99163

Attention:
Professor George Duvall
Professor G. R. Fowles
Professor Y. M. Gupta

Dr. J. Forbes, R13
U.S. Naval Surface Warfare Center
White Oak Laboratory
Silver Springs, MD 20903-5000

NASA, Marshall Space Flight Center
ED52 Structural Development Branch
Huntsville, AL 35812

Attention:
Mr. Scott A. Hill
Dr. Pedro Rodriguez
Mr. Joel Williamsen

Dr. David M. Jerome
Senior Research Engineer
AFATL/SAA
Eglin Air Force Base, FL 32542-5434

Dr. M. Scharff
Science Applications Inc.
Mail Stop 35
10260 Campus Point Dr.
San Diego, CA 92121

Dr. W. J. Tedeschi
Defense Nuclear Agency
Shock Physics/Special Projects
6801 Telegraph Road
Alexandria, VA 22310-3398

Dr. N. Thomas Tsai
Defense Nuclear Agency
Shock Physics Directorate
6801 Telegraph Road
Alexandria, VA 22310-3398

Lawrence Livermore National Lab.
P. O. Box 808
Livermore, CA 94550
Attention:
Dr. N. C. Holmes, L-387
Dr. W. J. Nellis, L-355
Dr. M. Ross, L-355
Dr. D. J. Steinberg, L-35
Dr. M. VanThiel, L-387

The Boeing Co.
P.O. Box 3999, Mail Stop 87-60
Seattle, WA 98124
Attention:
Mr. R. M. Schmidt
Dr. J. Shrader
Dr. E. Wilhelm

Sandia Internal:

0430 J. J. Bertin
1150 G. A. Samara
1153 M. Boslough
1153 R. A. Graham
1153 B. W. Dodson
1200 J. P. VanDevender
1201 M. J. Clauser
1500a L. W. Davison
1510 J. C. Cummings
1540 J. R. Asay

1541 J. M. McGlaun
1541 A. C. Robinson
1541 T. G. Trucano
1541 E. S. Hertel
1542 P. Yarrington
1542 J. E. Dunn
1542 G. I. Kerley
1542 M. E. Kipp
1542 J. S. Rottler
1543 P. L. Stanton
1543 L. C. Chhabildas (25)
1543 D. E. Cox
1543 M. D. Furnish
1543 D. E. Grady
1543 C. A. Hall
1543 C. H. Konrad
1543 R. McIntosh
1543 J. M. Miller
1543 R. L. Moody
1543 W. D. Reinhart
1543 J. W. Swegle
1543 M. Shahinpoor
1543 J. L. Wise
1544 J. R. Asay, Actg.
1545 D. R. Martinez
1550 C. W. Peterson
1600 W. Hermann
2513 D. B. Mitchell
2514 L. Bonzon
3141 S. A. Landenberger (5)
3151 G. L. Esch, Actg. (3)
3145 Document Processing DOE/OSTI (8)
5160 G. R. Otey
5165 J. F. Cuderman
5166 R. E. Setchell
8523 R. C. Christman
8400 R. C. Wayne
9143 E. W. Reece
9143 D. N. Benton
9143 R. Weir